

## Article

# Synthesis and Photostability of Cyclooctatetraene-Substituted Free Base Porphyrins

Joanna Buczyńska<sup>1</sup>, Agnieszka Gajewska<sup>1</sup>, Aleksander Gorski<sup>1</sup>, Barbara Golec<sup>1</sup>, Krzysztof Nawara<sup>1,2</sup>,  
Renata Rybakiewicz<sup>2</sup> and Jacek Waluk<sup>1,2,\*</sup>

<sup>1</sup> Institute of Physical Chemistry, Polish Academy of Sciences, Kasprzaka 44/52, 01-224 Warsaw, Poland; jrbuczynska@ichf.edu.pl (J.B.); agajewska@ichf.edu.pl (A.G.); agorski@ichf.edu.pl (A.G.); bgolec@ichf.edu.pl (B.G.); k.nawara@uksw.edu.pl (K.N.)

<sup>2</sup> Faculty of Mathematics and Science, Cardinal Stefan Wyszyński University, Dewajtis 5, 01-815 Warsaw, Poland; r.rybakiewicz@uksw.edu.pl

\* Correspondence: jwaluk@ichf.edu.pl; Tel.: +48-22-343-3332

**Abstract:** A series of free base *meso*-tetraarylporphyrins functionalized with substituents containing one, two, and four cyclooctatetraene (COT) moieties have been obtained and characterized by spectral and photophysical studies. Three COT-free porphyrins served as reference compounds. COT is a triplet quencher, well-known to enhance the photostability of several, but not all, fluorophores. In the case of porphyrins, substitution with COT improves photostability in zinc derivatives, but for free bases, the effect is the opposite. We show that placing the COT moiety further from the free base porphyrin core enhances the photostability when the COT group lies in the direct vicinity of the macrocycle. The quantum yields of photobleaching inversely correlate with porphyrin oxidation potentials. An improvement in photostability in both COT-containing and COT-free porphyrins can be achieved by screening the porphyrin core from oxygen by switching from tolyl to mesityl substituents. This leads to a decrease in the photobleaching quantum yield, even though triplet lifetimes are longer. The results confirm the involvement of oxygen in the photodegradation of porphyrins.

**Keywords:** photostability; photobleaching; porphyrins; self-healing fluorophores



**Citation:** Buczyńska, J.; Gajewska, A.; Gorski, A.; Golec, B.; Nawara, K.; Rybakiewicz, R.; Waluk, J. Synthesis and Photostability of Cyclooctatetraene-Substituted Free Base Porphyrins.

*Chemistry* **2021**, *3*, 104–115.

<https://doi.org/10.3390/chemistry3010008>

Received: 31 December 2020

Accepted: 17 January 2021

Published: 21 January 2021

**Publisher's Note:** MDPI stays neutral with regard to jurisdictional claims in published maps and institutional affiliations.



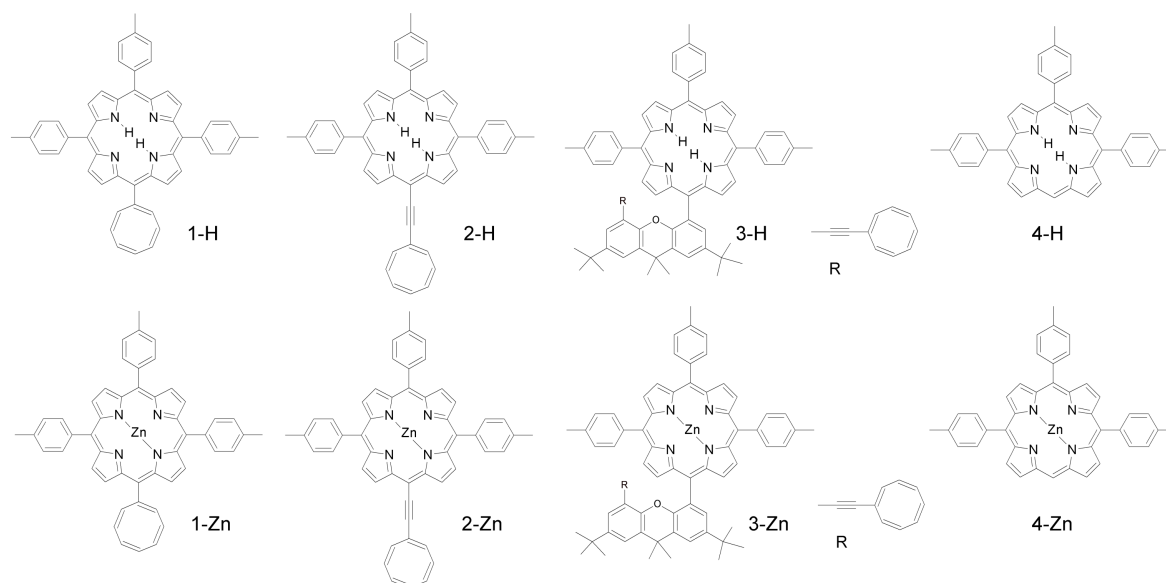
**Copyright:** © 2021 by the authors. Licensee MDPI, Basel, Switzerland. This article is an open access article distributed under the terms and conditions of the Creative Commons Attribution (CC BY) license (<https://creativecommons.org/licenses/by/4.0/>).

## 1. Introduction

The development of such widely used methodologies as fluorescence imaging, probing, sensing, and various single-molecule techniques relies on the rational synthesis of new fluorophores. Among various factors that should be taken into account while designing such materials, photostability plays a crucial role [1–5]. An excited molecule is usually more reactive than in the ground electronic state. It can also initiate production of reactive intermediates, for example, reactive oxygen species. This usually occurs via the lowest triplet state. Therefore, a strategy often used to enhance photostability is to shorten the triplet lifetime. This can be done by adding an external triplet quencher (TQ), acting via energy or electron transfer or by chemically attaching the quencher to the fluorophore. The latter approach leads to the so-called “self-healing chromophores” [6–31]. It has been demonstrated that linking a chromophore with TQs, such as cyclooctatetraene (COT), nitrobenzyl alcohol (NBA), Trolox (TX), nitrophenylalanine (NPA), or Ni(II) complex of *tris*-*N*-nitritoltriacetic acid (NTA), results in a substantial improvement in the photostability of various fluorophores.

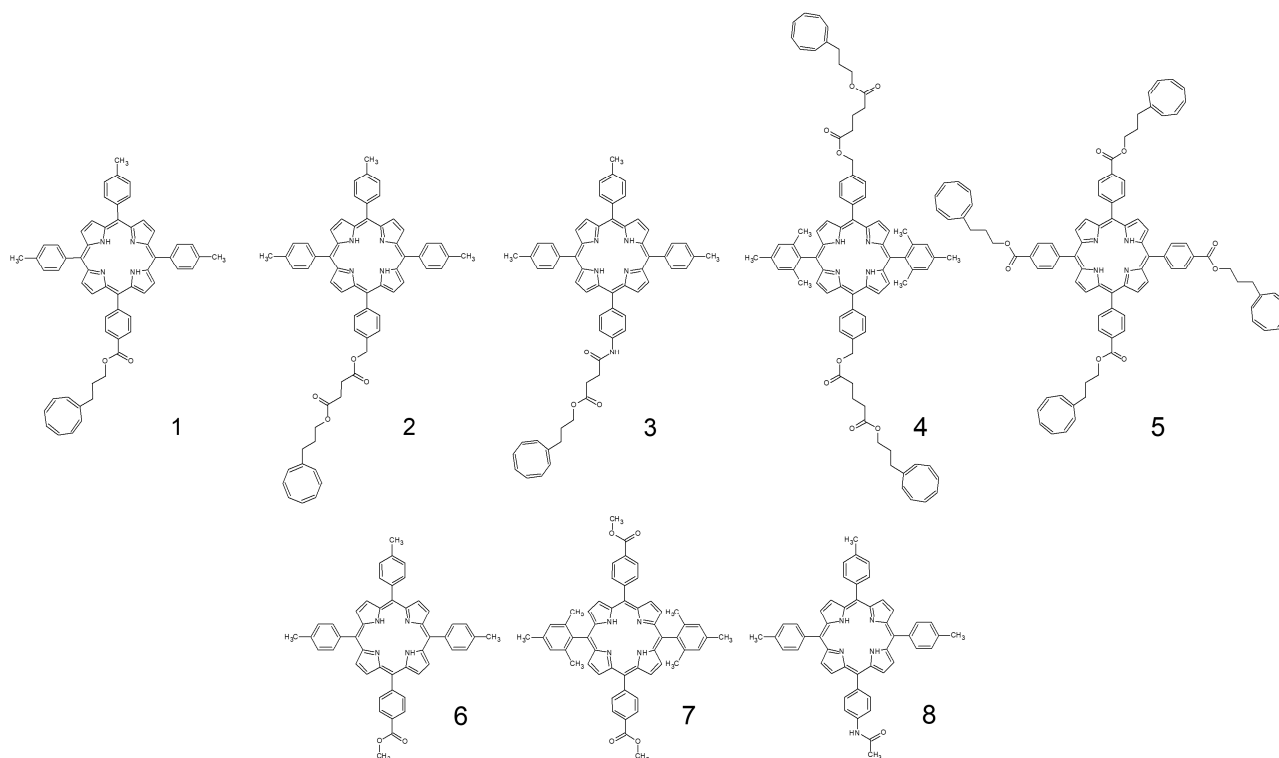
However, it is known [29] that the protective role of various triplet quenchers is not universal. In a recent study, we looked for photostability improvement in a series of free base and zinc porphyrins substituted with COT (Scheme 1) [32]. A significant enhancement (10-fold for aerated solutions, 3 orders of magnitude for deoxygenated ones) was found for the zinc porphyrins. On the other hand, the photostability of free bases decreased after substitution, becoming similar to that of zinc-COT porphyrins. This observation suggests a

common mechanism of photobleaching, such as photoinduced electron transfer between the porphyrin and COT subunits.



**Scheme 1.** Porphyrins investigated previously [32].

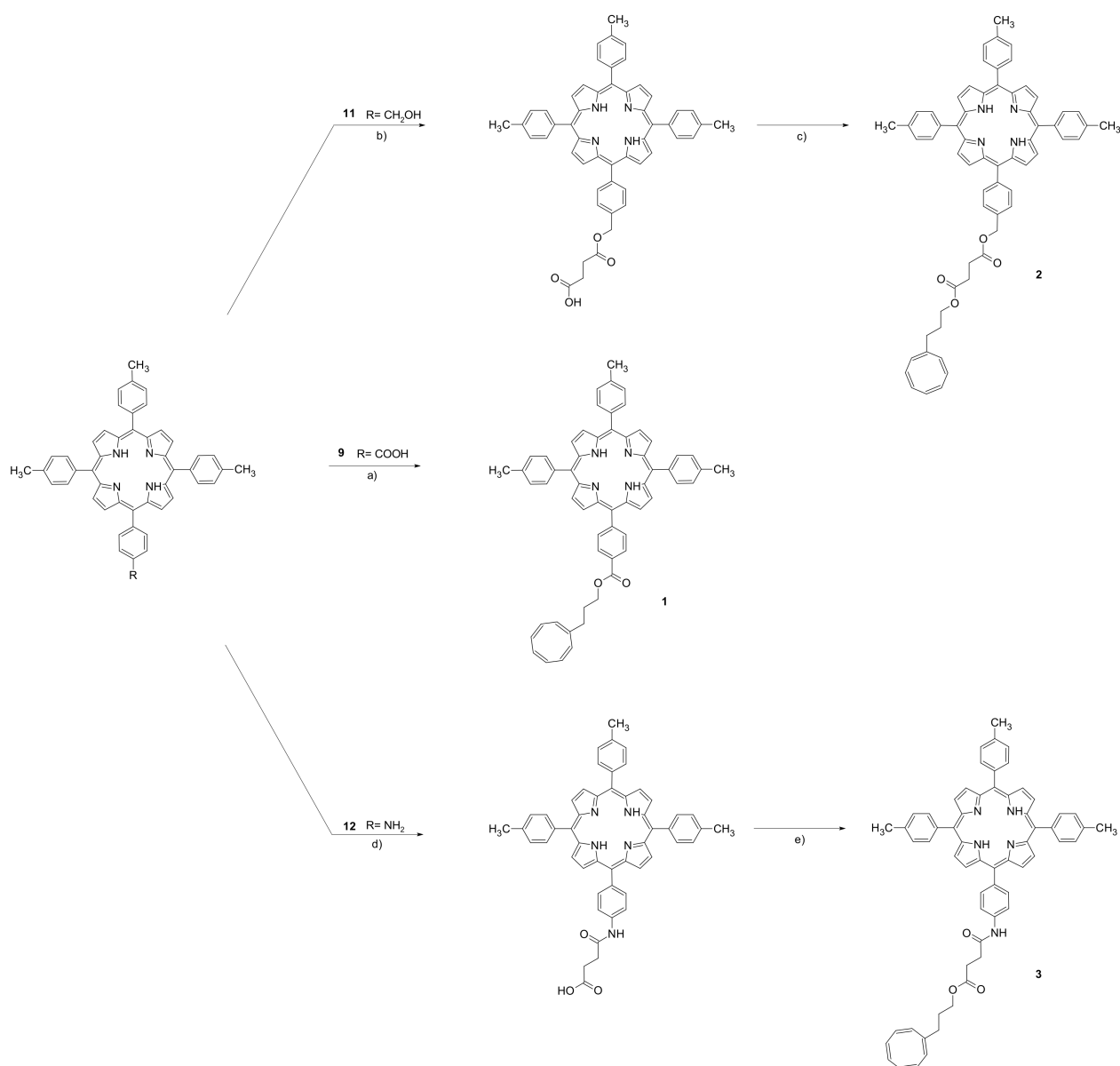
In this work, we focused on the photostability of eight novel free base porphyrins (Scheme 2); five of them contain the COT moiety, located at a larger distance from the porphyrin than the previously studied derivatives. This should lead to a decrease of the triplet quenching ability, but also to lower rates of photoinduced electron transfer. Our goal was to find out how such a combination of counteracting factors would influence photostability.



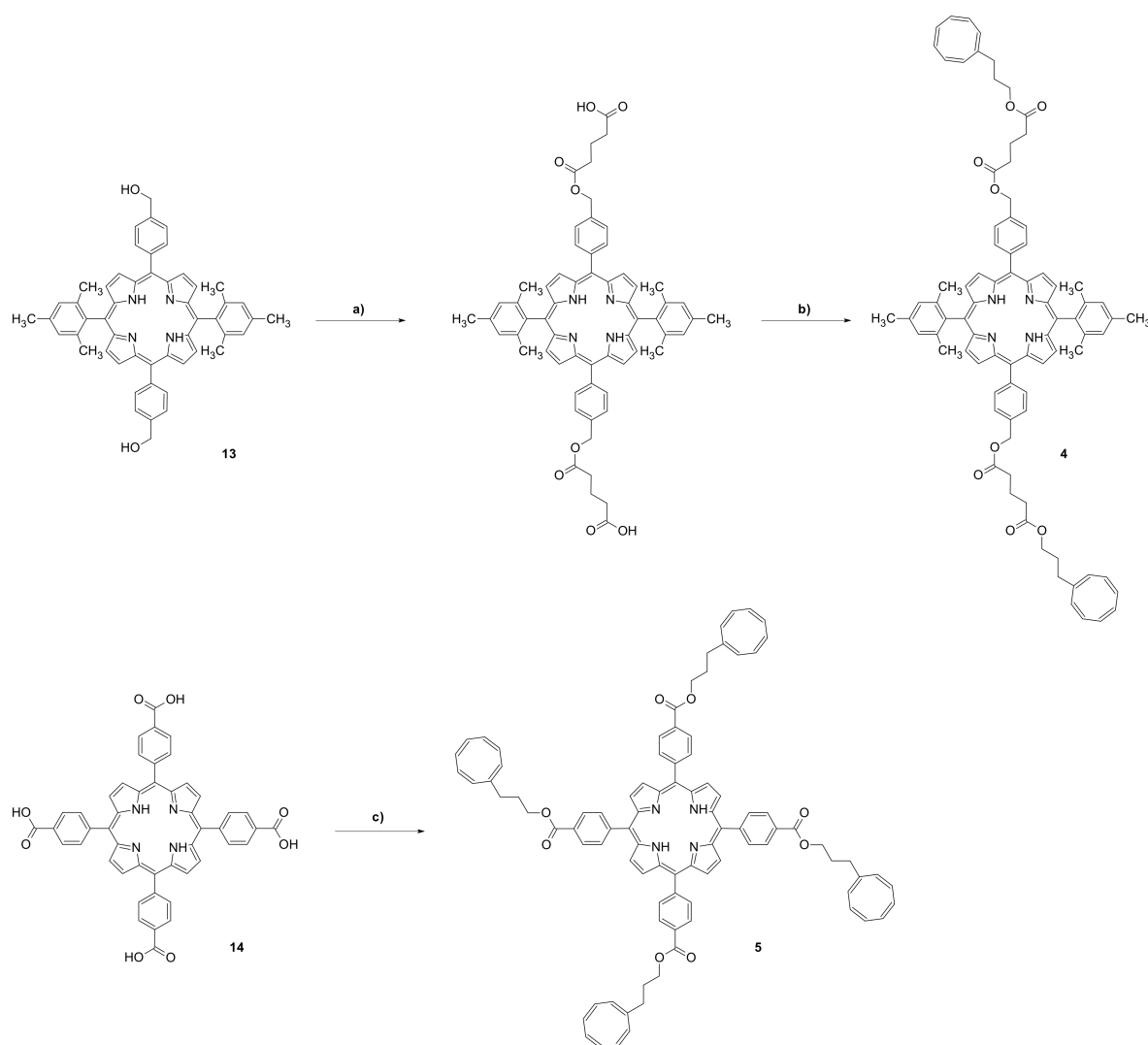
**Scheme 2.** Porphyrins investigated in this work.

## 2. Materials and Methods

The syntheses relied on the standard convergent strategy employing appropriate porphyrin- and COT-containing building blocks, which were linked by an ester or amide bond using succinic or glutaric anhydride. We report the preparation of three new porphyrins covalently bonded with one COT moiety (1–3, Scheme 3) and two more (4–5) containing more than one COT moiety (Scheme 4). The triplet state quencher was spaced by 5 to 11 atoms away from the porphyrin core. The syntheses of 1–8 are described in more detail in the Supplementary Materials.



**Scheme 3.** Syntheses of porphyrins containing one cyclooctatetraene (COT) moiety. Reagents and conditions: **(a)** 1,3,5,7-cyclooctatetraene-1-propanol (COT-OH), 4-DMAP, EDCI.Cl, anhydrous THF, rt, overnight; 49%. **(b)** succinic anhydride, Et<sub>3</sub>N, anhydrous DCM, rt, 16 h; 48%. **(c)** COT-OH, 4-DMAP, EDCI.Cl, anhydrous THF, rt, overnight; 55% **(d)** succinic anhydride, Et<sub>3</sub>N, anhydrous DCM, rt, 16 h; 83%. **(e)** COT-OH, 4-DMAP, EDCI.Cl, anhydrous THF, rt, overnight; 53%.



**Scheme 4.** Syntheses of porphyrins containing more than one COT moiety. Reagents and conditions: (a) glutaric anhydride, Et<sub>3</sub>N, anhydrous DCM, rt, 16 h; 92%. (b) COT-OH, 4-DMAP, EDCI.Cl, anhydrous THF, rt, overnight; 28% (c) COT-OH, 4-DMAP, EDCI.Cl, anhydrous THF, rt, overnight; 6%.

The triplet state lifetimes were measured using a home-built laser flash photolysis setup. An Oportek Radiant 355 laser (210–2500 nm tuning spectral region, 5 ns pulsewidth, 10 Hz repetition rate) was used as the excitation source. The continuous output of a laser-driven Xe lamp (Energetiq EQ-99-Plus-EU) was used as a probe. The setup was equipped with a Hamamatsu (Hamamatsu City, Japan) R955 photomultiplier and a Yokogawa (Tokyo, Japan) DL9140 fast oscilloscope. The samples were deaerated before measurements by a freeze–pump–thaw method. At least 6 freeze–pump–thaw cycles were done before each experiment. A low concentration of the investigated compounds, about  $5 \times 10^{-7}$  M, was used in order to avoid triplet–triplet annihilation.

Spectral grade toluene (Merck, Uvasol, Darmstadt, Germany) was used to prepare all the solutions. The electronic absorption spectra were measured with a Shimadzu UV 3100 spectrophotometer. The fluorescence spectra were obtained using an Edinburgh FS900 CDT or FS5 spectrofluorimeters. The fluorescence quantum yields were determined using *meso*-tetraphenylporphyrin in toluene as a standard ( $\Phi_{fl} = 0.10$  [33]).

Fluorescence lifetimes were determined using a homebuilt setup consisting of a Fianium FemtoPower1060 supercontinuum laser (6 ps pulses, tunable wavelength) as the excitation source, a Digikröm CM112 monochromator, a Becker & Hickl HPM-100-40 hybrid detector, and a Becker & Hickl SPC-830 time-correlated single-photon-counting

module. Fluorescence decays were analyzed using the SPCM software (Becker & Hickl, Berlin, Germany).

The procedure used to determine the photobleaching quantum yield ( $\Phi_{pb}$ ) is described in detail in the supporting information. Briefly, the values of  $\Phi_{pb}$  were obtained from the plots of  $A_0/A(t)$  vs.  $F(t)$ , where  $A_0$  and  $A(t)$  correspond to the absorbances measured before and after irradiation over time  $t$ , and  $F(t) = N_{total}(t)/A(t)$ .  $N_{total}(t)$  is the total number of photons absorbed by the substrate. The slope of the  $A_0/A(t)$  vs.  $F(t)$  plot is proportional to the photobleaching quantum yield (cf. also Figure 3).

The measurements of  $\Phi_{\Delta}$ , the quantum yield of singlet oxygen generation ( $^1O_2$ , emission at  $\lambda_{max} = 1275$  nm), were performed with a home-made experimental setup based on a BENTHAM DTMc300 double monochromator, equipped with a thermoelectrically cooled photomultiplier (Hamamatsu H10330C-75, 950–1700 nm registration range). The Oportek Radiant 355 laser was used for excitation, with phenalenone as the standard ( $\Phi_{\Delta}^0 = 0.99$  in toluene at ambient temperature [34]). The measurement of  $\Phi_{\Delta}$  was based on the comparison of amplitudes of singlet oxygen phosphorescence decay curves (measured at 1275 nm) photosensitized by a standard compound (amplitude  $Am_0$ ) and by the compound under investigation (amplitude  $Am_x$ ) in the same solvent:  $\Phi_{\Delta} = \Phi_{\Delta}^0 \times Am_x \times (1 - 10^{-OD_0}) / (Am_0 \times (1 - 10^{-OD_x}))$ , where  $1 - 10^{-OD_0}$  and  $1 - 10^{-OD_x}$  are fractions of exciting light absorbed by the standard and the sample, respectively, at a given excitation wavelength. The optical density (OD) of solutions did not exceed 0.1 at the optical length of 1 cm. The accuracy in the estimation of singlet oxygen emission quantum yield was estimated as 10%.

BioLogic Science Instruments (EC-Lab) were used for all electrochemical studies. The voltamperometric experiments were performed in a one-compartment three-electrode electrochemical cell with a platinum counter electrode (1.6 mm diameter) and an Ag quasi-reference electrode. The studied compound concentration was  $5 \times 10^{-4}$  M in an electrolyte consisting of 0.1 M  $Bu_4N(PF_6)$  dissolved in dichloromethane.

Calculations of the ground state geometries were performed using density functional theory (DFT), with the B3LYP functional and 6-31G(d)+ basis set, as implemented in the Gaussian 16 software package [35].

### 3. Results

Figure 1a shows the absorption of 1–8. The spectra are very similar, regarding both the positions of the maxima and the transition intensities (Table 1). The similarity is also preserved in the emission (Figure 1b and Table 1). The fluorescence quantum yields are practically the same, given the experimental accuracy of about 20%. The decay times differ by less than 20%. It can be therefore assumed that the other spectral and photophysical characteristics, such as the energy of the lowest triplet state and triplet formation efficiency are also very similar in the whole series. In other words, modifying the structure of *meso*-tetra-*p*-tolylporphyrin by the substituents shown in Scheme 2 does not significantly affect the spectral and photophysical parameters. This is opposite to the behavior of the previously studied COT-substituted porphyrins shown in Scheme 1. In these molecules, placing the COT moiety very close to the porphyrin core resulted in spectral shifts in absorption and emission, as well as a decrease in fluorescence lifetimes and quantum yields [32].

It is known that the photodegradation of *meso*-tetraarylporphyrins in toluene occurs by different mechanisms in aerated and in deoxygenated solutions [36]. In the present work, we used “normal” conditions, that is, non-degassed solutions for the studies of photostability. However, triplet lifetimes were measured in both regimes, in order to separate the intrinsic and oxygen-induced rates of triplet decay (Tables 1 and 2). Figure 2 shows the evolution of the spectra of porphyrin 1 observed upon irradiation. The absorption in the whole visible region gradually decreased, without the appearance of new bands. A rising absorption was only observed below 340 nm. Figure 3 shows the plots of  $A_0/A(t)$  vs.  $F(t)$ , from which the photobleaching quantum yields could be determined. Except for porphyrins 4 and 7, these plots are linear. Such behavior indicates that (i) there was no interference due to the absorption from species other than the substrate, and (ii) the

photons from the light source used for irradiation were exclusively absorbed by the initial porphyrin during the whole experiment.

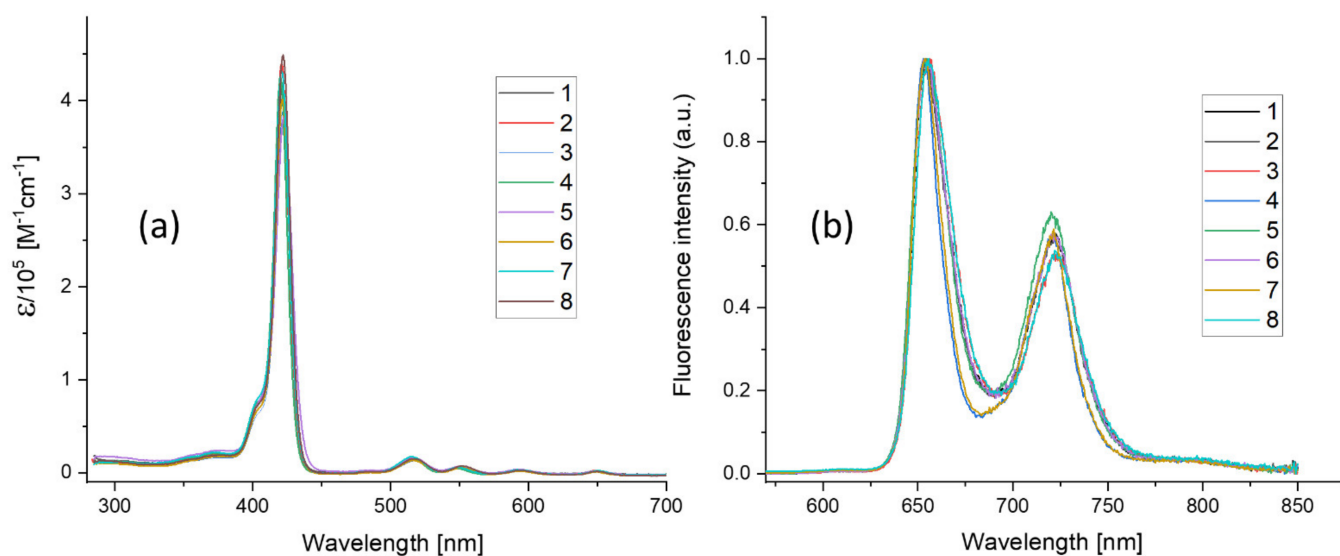


**Figure 1.** (a) Absorption spectra; (b) normalized fluorescence spectra of 1–8 (toluene, 293 K).

**Table 1.** Spectral and photophysical parameters. Toluene solutions, 293 K.

	Abs. Maxima [nm]	Abs. Coeff [ $M^{-1} cm^{-1}$ ]	$\Phi_{fl}$	$S_1$ Lifetime [ns]	$T_1$ Lifetime Aerated [ns]	$T_1$ Lifetime Degassed [ $\mu s$ ]	$\Phi_{\Delta}$	$\Phi_{pb}$
1	421	416,860	0.12	9.7	293	458	0.78	$4.9 \times 10^{-7}$
	516	17,558						
	551.5	9056						
	593.5	5016						
	649.5	3901						
2	420.5	440,270	0.12	9.6	297	14.7	0.7	$7.0 \times 10^{-7}$
	516	17,921						
	551	9077						
	592.5	5035						
	648.5	4014						
3	421.5	389,104	0.12	9.5	298	112	0.75	$7.7 \times 10^{-7}$
	517	15,590						
	552	8793						
	594	4486						
	649.5	3872						
4	420	426,346	0.13	10.3	386	9.3	0.72	$2.5 \times 10^{-7}$
	514.5	18,376						
	548	7350						
	591.5	5052						
	650	4380						
5	422	383,662	0.13	10.2	329	257	0.66	$3.9 \times 10^{-7}$
	516	15,931						
	550.5	7171						
	593	4281						
	649	2949						

Table 1. Cont.

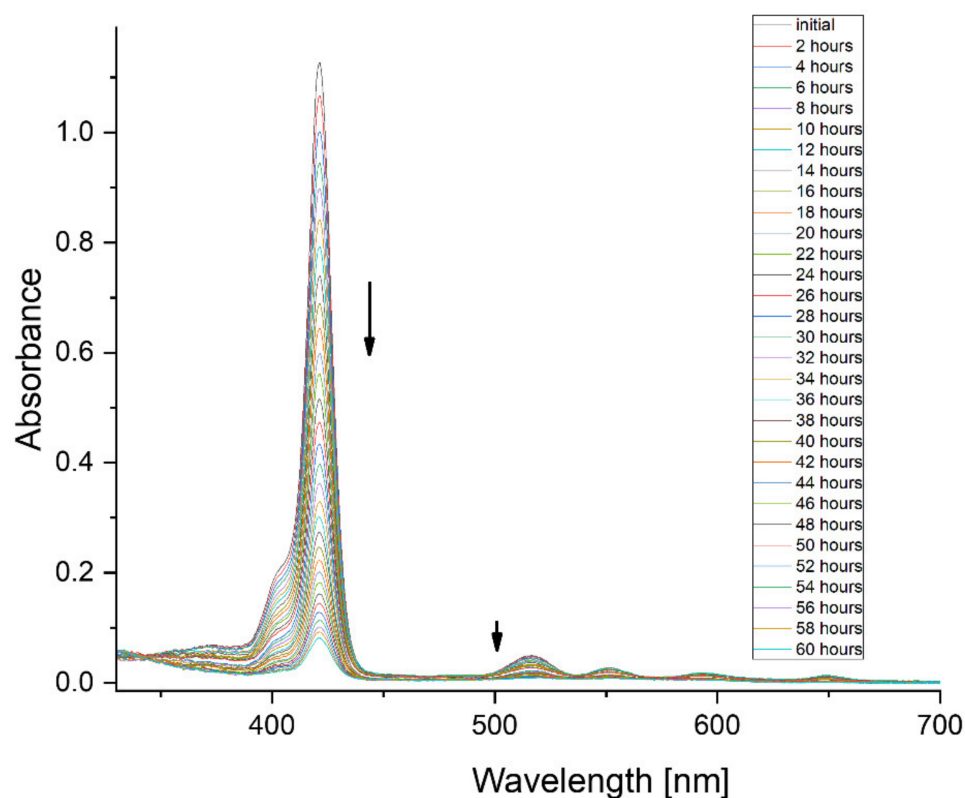
6	421	401,207	0.12	9.6	297	645	0.78	$4.8 \times 10^{-7}$
	516	16,709						
	551	8627						
	593.5	4795						
	649.5	3735						
7	420.5	431,582	0.14	10.4	509	1070	0.78	$7.1 \times 10^{-8}$
	515	20,127						
	548.5	8252						
	592.5	5515						
	650.5	4621						
8	421.5	449,392	0.13	9.5	294	820	0.79	$4.5 \times 10^{-7}$
	517	15,922						
	552.5	8839						
	593.5	4545						
	650.5	3849						

The lack of absorption of the photoproduct in the visible range can be explained by the mechanism of photodestruction of *meso*-tetraphenylporphyrins proposed in the literature [37–41]. It involves the breaking of the macrocycle by an oxygen molecule, resulting in the formation of a noncyclic tetrapyrrolic structure. The latter should not absorb in the visible range.

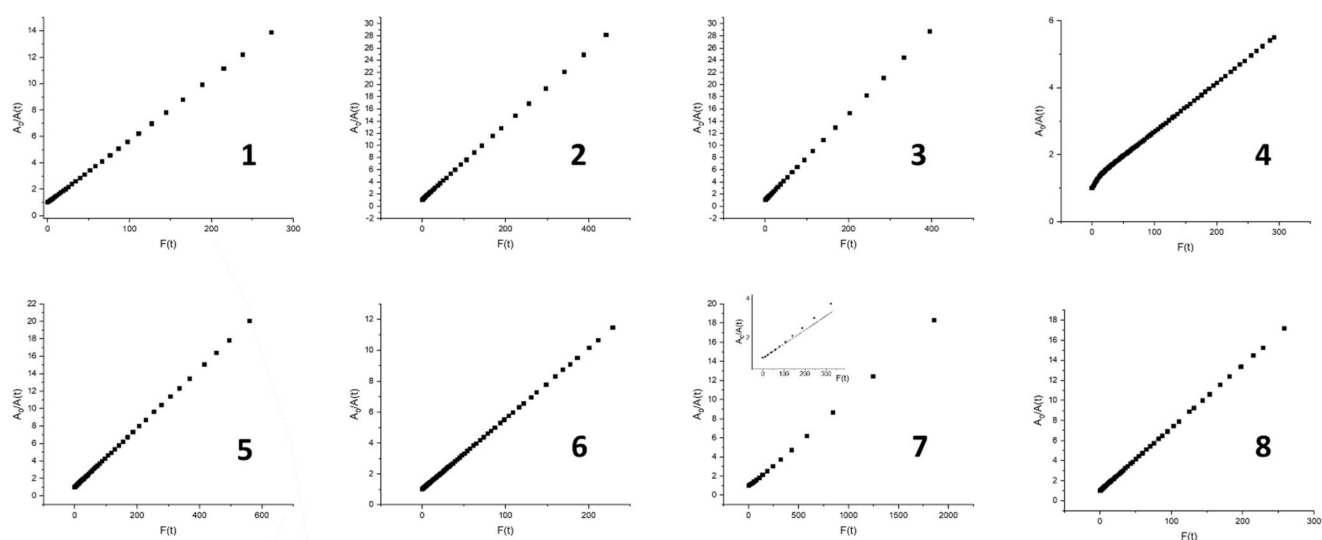
Porphyrins 4 and 7 revealed a different behavior, evidenced by the nonlinearity of the plots presented in Figure 3. Closer inspection of the absorption spectra reveals that the overall decrease was also accompanied by small (2–3 nm) spectral shifts of the Q bands (blue shift for the lower energy Q<sub>x</sub> band and the red shift of the Q<sub>y</sub> band). This finding indicates that the macrocycle was somehow modified before being broken. It should be noted that for the previously studied free base porphyrins bearing the COT substituent (1-H, 2-H, and 3-H), the  $A_0/A(t)$  vs.  $F(t)$  plots were nonlinear, while for 4-H, a porphyrin without COT, perfect linearity was obtained. These results demonstrate the more complex photochemistry of COT-containing porphyrins, possibly involving the photoinduced transformation of the COT group.

Table 2. Rate constants of intramolecular and oxygen-induced triplet decay.

Compound	$k_{intr}$ [ $10^6 \text{ s}^{-1}$ ]	$k_q[\text{O}_2]$ [ $10^6 \text{ s}^{-1}$ ]
1-H	5.6	3.8
2-H	5.4	7.6
3-H	5.2	6.8
4-H	0.0048	4
1-Zn	5.6	4.1
2-Zn	5.2	7.8
3-Zn	17	4
4-Zn	0.0038	2.8
1	0.0022	3.4
2	0.068	3.4
3	0.0089	3.4
4	0.11	2.5
5	0.0039	3
6	0.0016	3.4
7	0.00093	2
8	0.0012	3.4



**Figure 2.** Changes in the absorption of porphyrin 1 observed upon irradiation. The sample was irradiated for 60 h, using an LED emitting at 420 nm (63 mW).



**Figure 3.** The ratio of the initial absorption,  $A_0$ , to the absorption recorded after irradiating for time  $t$ ,  $A(t)$ , vs.  $F(t)$ , obtained for the toluene solutions of porphyrins 1–8 at 293 K. The monitoring wavelengths correspond to the absorption maxima (see Table 1). The inset shows deviation from linearity in the initial period of irradiation of porphyrin 7.

Contrary to the other photophysical parameters, clear differences were observed regarding photostability. The values of the photobleaching quantum yields of porphyrins 1–8 (Table 1) vary by an order of magnitude, spanning the range from  $7.1 \times 10^{-8}$  to  $7.7 \times 10^{-7}$ . The most stable porphyrin 7, does not contain the COT substituent. This was also the case for the series of 1-H, 2-H, 3-H, and 4-H, which revealed the photobleaching quantum yields of  $5.6 \times 10^{-6}$ ,  $1.7 \times 10^{-6}$ ,  $1.1 \times 10^{-6}$ , and  $2.2 \times 10^{-7}$ , respectively. However,

in the present series, the next most stable porphyrin, 4, does contain the COT units. Its photostability is about two times better than that of the two other porphyrins without COT substituents: 6 and 8.

#### 4. Discussion

It is remarkable and, at first, counterintuitive that the two most stable porphyrins, 7 and 4, reveal the longest  $T_1$  lifetimes (509 and 386 ns, respectively), while the  $T_1$  states of the remaining six porphyrins decay in less than 300 ns. It is often assumed that the photostability should be enhanced for shorter triplet lifetimes. In the present case, the “unusual” behavior can be understood upon close inspection of the structures (Scheme 2). Porphyrins 4 and 7 are the only ones that have mesityl, and not tolyl, substituents at positions 10 and 20. This may lead to the “screening” of the chromophore from oxygen, which results in less efficient quenching and, thus, longer  $T_1$  decay. Moreover, the screened chromophore is better protected against oxidation. These findings also provide strong arguments for the involvement of oxygen in porphyrin photodegradation.

One should notice that the quantum yields of singlet oxygen formation in porphyrins 1–8 are equal within experimental error. Thus, the steric factor may be important for the photoinduced reaction, but not for physical quenching of the lowest triplet state of the porphyrin.

The enhancement of photostability in 2,6-substituted *meso*-tetraphenylporphyrin derivatives has been observed and discussed before [42]. The authors concluded that “the steric effects in protecting the macrocycle seem to be predominant over the electronic ones”. In the present case, it may not be true, even though the steric effect is clearly seen. If thermodynamics, not kinetics, is the governing factor in photooxidation, one should expect the correlation between the photodegradation quantum yield and the ionization potential. As a measure of the latter, we used the calculated energy values of the highest occupied molecular orbital (HOMO). Their ordering was found to be in reasonable agreement with the ionization potentials estimated from cyclic voltammetry data (Table S2). Figure 4 shows that, except for one compound (5), the correlation between  $\Phi_{pb}$  and E(HOMO) is indeed obtained. Porphyrin 5 reveals much lower photostability than expected from this correlation. We note that this is the only derivative with four COT moieties, which may suggest photochemistry involving the latter. It is supported by the finding that no correlation could be obtained between the photobleaching quantum yields and the HOMO values calculated for 1-H-4-H and 1-Zn-4-Zn.

Comparison of the triplet lifetimes of porphyrins 1–8 in aerated solutions (Table 1) with the corresponding values for the previously studied series [32] clearly shows that placing the COT group further from the porphyrin core leads to the behavior typical for porphyrins that do not contain the triplet quencher. The rate of porphyrin  $T_1$  decay can be expressed as  $k_{intr} + kq[O_2]$ , where the first term is the sum of all intramolecular channels, including quenching by COT. The two terms can be separated by comparing the triplet decays measured in aerated and degassed solutions. Table 2 presents the results. The effect is dramatic. In molecules with COT close to porphyrin, the intramolecular decay channel can compete with oxygen quenching, becoming the fastest depopulation route in 1-H, 1-Zn, and 3-Zn. In contrast, for porphyrins 1–8, the intramolecular channel is about three orders of magnitude slower, and thus, completely dominated by the intermolecular process, even though the oxygen quenching rates are somewhat lower, most probably due to steric hindrance. Intramolecular triplet quenching is observed in two COT-containing porphyrins, 2 and 4, that exhibit  $T_1$  decay times of ca. 10  $\mu$ s in degassed solutions (Table 1), but this is not enough to effectively compete with quenching by oxygen.

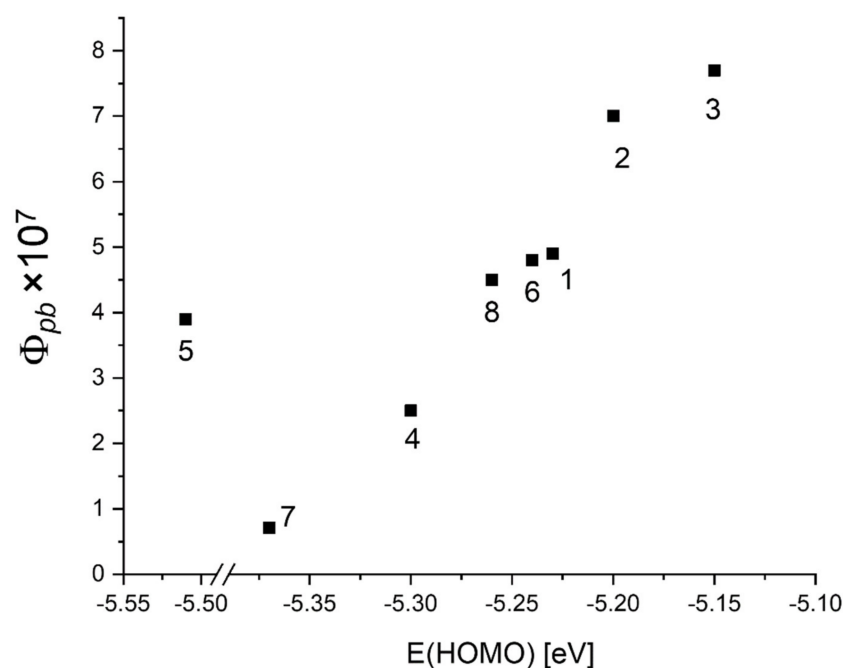


**Figure 4.** Correlation between the observed photobleaching quantum yields and the calculated highest occupied molecular orbital (HOMO) energies.

The photobleaching quantum yields of porphyrins 1–8 in aerated solutions are, in all cases, lower than the corresponding values obtained for porphyrins 1-H, 2-H, and 3-H. This observation demonstrates that very efficient intramolecular triplet quenching, leading to the population of the COT triplet, results in a decrease of photostability in aerated solutions. We anticipate that this ordering will be reversed for deoxygenated solutions, based on the finding that 1-H, 2-H, and 3-H become 10 to 20 times more photostable when oxygen is removed [32]. If this is the case, it could suggest the oxidation of  $^3\text{COT}$  as the degradation route. However, in order to fully exploit the “self-healing” potential of COT-substituted porphyrins, one has to understand, in detail, the photobleaching mechanisms. Our results show different responses to the peripheral and direct attachment of COT to the macrocycle and, in particular, to the extent of conjugation between COT and porphyrin. It has been suggested that the competition between energy and electron transfer may be the reason for the low responsiveness of some fluorophore to COT [19]. In the case of porphyrins, initial estimates indicate that the electron transfer between the  $T_1$  state of the porphyrin and COT seems to be thermodynamically uphill. Most probably, the doorway to photobleaching is open after populating the COT triplet. We hope to determine the role of various energy relaxation channels by time-resolved spectroscopy of porphyrin–COT conjugates, as well as of COT alone. Such measurements are now in progress.

**Supplementary Materials:** The following are available online at <https://www.mdpi.com/2624-8549/3/1/8/s1>: Detailed synthetic procedures, the methodology of determination of photobleaching quantum yields, cyclic voltammetry data. Table S1: Cyclic voltammetry data, Table S2. Experimentally determined ionization potentials (IP), electron affinities (EA), and energy gaps (Eg).

**Author Contributions:** A.G. (Agnieszka Gajewska) synthesized and purified the compounds. A.G. (Aleksander Gorski), J.B. and K.N. performed the spectral and photophysical studies. J.B. and B.G. studied the photodegradation. R.R. did the electrochemical experiments. J.W. performed the calculations and wrote the initial draft of the manuscript, with input from all the authors. All authors have read and agreed to the published version of the manuscript.

**Funding:** This research was funded by the Polish National Science Centre, grant number 2016/22/A/ST4/00029.

**Institutional Review Board Statement:** Not applicable.

**Informed Consent Statement:** Not applicable.

**Data Availability Statement:** Data is contained within the article or supplementary materials.

**Acknowledgments:** We thank Jędrzej SolarSKI for the initial electrochemical measurements.

**Conflicts of Interest:** The authors declare no conflict of interest.

## References

1. Demchenko, A.P. Photobleaching of organic fluorophores: Quantitative characterization, mechanisms, protection. *Methods Appl. Fluoresc.* **2020**, *8*, 022001. [[CrossRef](#)] [[PubMed](#)]
2. Ha, T.; Tinnefeld, P. Photophysics of Fluorescent Probes for Single-Molecule Biophysics and Super-Resolution Imaging. *Ann. Rev. Phys. Chem.* **2012**, *63*, 595–617. [[CrossRef](#)] [[PubMed](#)]
3. Bregnhøj, M.; Prete, M.; Turkovic, V.; Petersen, A.U.; Nielsen, M.B.; Madsen, M.; Ogilby, P.R. Oxygen-dependent photophysics and photochemistry of prototypical compounds for organic photovoltaics: Inhibiting degradation initiated by singlet oxygen at a molecular level. *Methods Appl. Fluoresc.* **2019**, *8*, 014001. [[CrossRef](#)]
4. Grabenhorst, L.; Trofymchuk, K.; Steiner, F.; Glembockyte, V.; Tinnefeld, P. Fluorophore photostability and saturation in the hotspot of DNA origami nanoantennas. *Methods Appl. Fluoresc.* **2020**, *8*, 024003. [[CrossRef](#)]
5. Widengren, J.; Chmyrov, A.; Eggeling, C.; Löfdahl, P.-Å.; Seidel, C.A.M. Strategies to Improve Photostabilities in Ultrasensitive Fluorescence Spectroscopy. *J. Phys. Chem. A* **2007**, *111*, 429–440. [[CrossRef](#)]
6. Liphardt, B.; Lüttke, W. Laser-Dyes. I. Bifluorophoric Laser-Dyes for Increase of the Efficiency of Dye-Lasers. *Liebigs Ann. Chem.* **1981**, 1118–1138. [[CrossRef](#)]
7. Liphardt, B.; Liphardt, B.; Lüttke, W. Laser dyes with intramolecular triplet quenching. *Opt. Commun.* **1981**, *38*, 207–210. [[CrossRef](#)]
8. Schäfer, F.P.; Zhang, F.G.; Jethwa, J. Intramolecular TT-energy transfer in bifluorophoric laser dyes. *Appl. Phys. B* **1982**, *28*, 37–41. [[CrossRef](#)]
9. Altman, R.B.; Terry, D.S.; Zhou, Z.; Zheng, Q.; Geggier, P.; Kolster, R.A.; Zhao, Y.; Javitch, J.A.; Warren, J.D.; Blanchard, S.C. Cyanine fluorophore derivatives with enhanced photostability. *Nat. Methods* **2012**, *9*, 68–71. [[CrossRef](#)]
10. Tinnefeld, P.; Cordes, T. ‘Self-healing’ dyes: Intramolecular stabilization of organic fluorophores. *Nat. Methods* **2012**, *9*, 426–427. [[CrossRef](#)]
11. Altman, R.B.; Zheng, Q.; Zhou, Z.; Terry, D.S.; Warren, J.D.; Blanchard, S.C. Enhanced photostability of cyanine fluorophores across the visible spectrum. *Nat. Methods* **2012**, *9*, 428–429. [[CrossRef](#)] [[PubMed](#)]
12. Zheng, Q.; Jockusch, S.; Zhou, Z.; Altman, R.B.; Warren, J.D.; Turro, N.J.; Blanchard, S.C. On the Mechanisms of Cyanine Fluorophore Photostabilization. *J. Phys. Chem. Lett.* **2012**, *3*, 2200–2203. [[CrossRef](#)] [[PubMed](#)]
13. Van der Velde, J.H.M.; Ploetz, E.; Hiermaier, M.; Oelerich, J.; de Vries, J.W.; Roelfes, G.; Cordes, T. Mechanism of Intramolecular Photostabilization in Self-Healing Cyanine Fluorophores. *ChemPhysChem* **2013**, *14*, 4084–4093. [[CrossRef](#)] [[PubMed](#)]
14. Van der Velde, J.H.M.; Oelerich, J.; Huang, J.Y.; Smit, J.H.; Hiermaier, M.; Ploetz, E.; Herrmann, A.; Roelfes, G.; Cordes, T. The Power of Two: Covalent Coupling of Photostabilizers for Fluorescence Applications. *J. Phys. Chem. Lett.* **2014**, *5*, 3792–3798. [[CrossRef](#)]
15. Zheng, Q.; Juette, M.F.; Jockusch, S.; Wasserman, M.R.; Zhou, Z.; Altman, R.B.; Blanchard, S.C. Ultra-stable organic fluorophores for single-molecule research. *Chem. Soc. Rev.* **2014**, *43*, 1044–1056. [[CrossRef](#)]
16. Zheng, Q.; Jockusch, S.; Zhou, Z.; Blanchard, S.C. The Contribution of Reactive Oxygen Species to the Photobleaching of Organic Fluorophores. *Photochem. Photobiol.* **2014**, *90*, 448–454. [[CrossRef](#)]
17. Juette, M.F.; Terry, D.S.; Wasserman, M.R.; Zhou, Z.; Altman, R.B.; Zheng, Q.; Blanchard, S.C. The bright future of single-molecule fluorescence imaging. *Curr. Opin. Chem. Biol.* **2014**, *20*, 103–111. [[CrossRef](#)]
18. Van der Velde, J.H.M.; Uusitalo, J.J.; Ugen, L.J.; Warszawik, E.M.; Herrmann, A.; Marrink, S.J.; Cordes, T. Intramolecular photostabilization via triplet-state quenching: Design principles to make organic fluorophores “self-healing”. *Faraday Discuss.* **2015**, *184*, 221–235. [[CrossRef](#)]
19. Zheng, Q.S.; Jockusch, S.; Rodriguez-Calero, G.G.; Zhou, Z.; Zhao, H.; Altman, R.B.; Abruna, H.D.; Blanchard, S.C. Intra-molecular triplet energy transfer is a general approach to improve organic fluorophore photostability. *Photochem. Photobiol. Sci.* **2016**, *15*, 196–203. [[CrossRef](#)]
20. Van der Velde, J.H.M.; Oelerich, J.; Huang, J.; Smit, J.H.; Aminian Jazi, A.; Galiani, S.; Kolmakov, K.; Gouridis, G.; Eggeling, C.; Herrmann, A.; et al. A simple and versatile design concept for fluorophore derivatives with intramolecular photostabilization. *Nature Comm.* **2016**, *7*, 10144. [[CrossRef](#)]
21. Zheng, Q.; Jockusch, S.; Zhou, Z.; Altman, R.B.; Zhao, H.; Asher, W.; Holsley, M.; Mathiasen, S.; Geggier, P.; Javitch, J.A.; et al. Electronic tuning of self-healing fluorophores for live-cell and single-molecule imaging. *Chem. Sci.* **2017**, *8*, 755–762. [[CrossRef](#)] [[PubMed](#)]
22. Zheng, Q.; Lavis, L.D. Development of photostable fluorophores for molecular imaging. *Curr. Opin. Chem. Biol.* **2017**, *39*, 32–38. [[CrossRef](#)] [[PubMed](#)]
23. Minoshima, M.; Kikuchi, K. Photostable and photoswitching fluorescent dyes for super-resolution imaging. *JBIC J. Biol. Inorg. Chem.* **2017**, *22*, 639–652. [[CrossRef](#)] [[PubMed](#)]
24. Van der Velde, J.H.M.; Smit, J.H.; Hebisch, E.; Punter, M.; Cordes, T. Self-healing dyes for super-resolution fluorescence microscopy. *J. Phys. D Appl. Phys.* **2018**, *52*, 034001. [[CrossRef](#)]

25. Glembockyte, V.; Wieneke, R.; Gatterdam, K.; Gidi, Y.; Tampé, R.; Cosa, G. Tris-N-Nitrilotriacetic Acid Fluorophore as a Self-Healing Dye for Single-Molecule Fluorescence Imaging. *J. Am. Chem. Soc.* **2018**, *140*, 11006–11012. [[CrossRef](#)] [[PubMed](#)]
26. Li, T.; Liu, L.; Jing, T.; Ruan, Z.; Yuan, P.; Yan, L. Self-Healing Organic Fluorophore of Cyanine-Conjugated Amphiphilic Polypeptide for Near-Infrared Photostable Bioimaging. *ACS Appl. Mater. Interfaces* **2018**, *10*, 14517–14530. [[CrossRef](#)]
27. Gong, W.; Das, P.; Samanta, S.; Xiong, J.; Pan, W.; Gu, Z.; Zhang, J.; Qu, J.; Yang, Z. Redefining the photo-stability of common fluorophores with triplet state quenchers: Mechanistic insights and recent updates. *Chem. Comm.* **2019**, *55*, 8695–8704. [[CrossRef](#)]
28. Smit, J.H.; van der Velde, J.H.M.; Huang, J.; Trauschke, V.; Henrikus, S.S.; Chen, S.; Eleftheriadis, N.; Warszawik, E.M.; Herrmann, A.; Cordes, T. On the impact of competing intra- and intermolecular triplet-state quenching on photobleaching and photoswitching kinetics of organic fluorophores. *Phys. Chem. Chem. Phys.* **2019**, *21*, 3721–3733. [[CrossRef](#)]
29. Isselstein, M.; Zhang, L.; Glembockyte, V.; Brix, O.; Cosa, G.; Tinnefeld, P.; Cordes, T. Self-Healing Dyes—Keeping the Promise? *J. Phys. Chem. Lett.* **2020**, *11*, 4462–4480. [[CrossRef](#)]
30. Pati, A.K.; El Bakouri, O.; Jockusch, S.; Zhou, Z.; Altman, R.B.; Fitzgerald, G.A.; Asher, W.B.; Terry, D.S.; Borgia, A.; Holsley, M.D.; et al. Tuning the Baird aromatic triplet-state energy of cyclooctatetraene to maximize the self-healing mechanism in organic fluorophores. *Proc. Natl. Acad. Sci. USA* **2020**, *117*, 24305–24315. [[CrossRef](#)]
31. Yang, Z.; Li, L.; Ling, J.; Liu, T.; Huang, X.; Ying, Y.; Zhao, Y.; Zhao, Y.; Lei, K.; Chen, L.; et al. Cyclooctatetraene-conjugated cyanine mitochondrial probes minimize phototoxicity in fluorescence and nanoscopic imaging. *Chem. Sci.* **2020**, *11*, 8506–8516. [[CrossRef](#)]
32. Ostapko, J.; Gorski, A.; Buczyńska, J.; Golec, B.; Nawara, K.; Kharchenko, A.; Listkowski, A.; Ceborska, M.; Pietrzak, M.; Waluk, J. Towards More Photostable, Brighter, and Less Phototoxic Chromophores: Synthesis and Properties of Porphyrins Functionalized with Cyclooctatetraene. *Chem. Eur. J.* **2020**, *70*, 16666–16675. [[CrossRef](#)] [[PubMed](#)]
33. Pineiro, M.; Carvalho, A.L.; Pereira, M.M.; Gonsalves, A.M.A.R.; Arnaut, L.G.; Formosinho, S.J. Photoacoustic measurements of porphyrin triplet-state quantum yields and singlet-oxygen efficiencies. *Chem. Eur. J.* **1998**, *11*, 2299–2307. [[CrossRef](#)]
34. Schmidt, R.; Tanielian, C.; Dunsbach, R.; Wolff, C. Phenalenone, a universal reference compound for the determination of quantum yields of singlet oxygen O<sub>2</sub> (<sup>1</sup>Δ<sub>g</sub>) sensitization. *J. Photochem. Photobiol. A Chem.* **1994**, *79*, 11–17. [[CrossRef](#)]
35. Frisch, M.; Trucks, G.; Schlegel, H.; Scuseria, G.; Robb, M.; Cheeseman, J.; Scalmani, G.; Barone, V.; Petersson, G.; Nakatsuji, H.; et al. *Gaussian 16, Revision A.03*; Gaussian, Inc.: Wallingford, CT, USA, 2016.
36. Cavaleiro, J.A.S.; Görner, H.; Lacerda, P.S.S.; MacDonald, J.G.; Mark, G.; Neves, M.G.P.M.S.; Nohr, R.S.; Schuchmann, H.P.; van Sonntag, C.; Tome, A.C. Singlet oxygen formation and photostability of meso-tetraarylporphyrin derivatives and their copper complexes. *J. Photochem. Photobiol. A Chem.* **2001**, *144*, 131–140. [[CrossRef](#)]
37. Cavaleiro, J.A.S.; Hewlins, M.J.E.; Jackson, A.H.; Neves, G.P.M.S. Structures of the Ring-Opened Oxidation Products from meso-Tetraphenylporphyrins. *J. Chem. Soc. Chem. Comm.* **1986**, 142–144. [[CrossRef](#)]
38. Cavaleiro, J.A.S.; Neves, M.G.P.S.; Hewlins, M.J.E.; Jackson, A.H. The Photooxidation of Meso-Tetraphenylporphyrins. *J. Chem. Soc. Perkin Trans. 1* **1990**, *7*, 1937–1943. [[CrossRef](#)]
39. Smith, K.M.; Brown, S.B.; Troxler, R.F.; Lai, J.J. Mechanism of photo-oxygenation of meso-tetraphenylporphyrin metal complexes. *Tetrahedron Lett.* **1980**, *21*, 2763–2766. [[CrossRef](#)]
40. Smith, K.M.; Brown, S.B.; Troxler, R.F.; Lai, J.J. Photooxygenation of meso-tetraphenylporphyrin complexes. *Photochem. Photobiol.* **1982**, *36*, 147–152. [[CrossRef](#)]
41. Wojaczyński, J.; Popiel, M.; Szterenber, L.; Latos-Grażyński, L. Common Origin, Common Fate: Regular Porphyrin and N-Confused Porphyrin Yield an Identical Tetrapyrrolic Degradation Product. *J. Org. Chem.* **2011**, *76*, 9956–9961. [[CrossRef](#)]
42. Silva, A.M.S.; Neves, M.G.P.M.S.; Martins, R.R.L.; Cavaleiro, J.A.S.; Boschi, T.; Tagliatesta, P. Photo-oxygenation of meso-tetraphenylporphyrin derivatives: The influence of the substitution pattern and characterization of the reaction products. *J. Porphyr. Phthalocyanines* **1998**, *2*, 45–51. [[CrossRef](#)]